Mir-290–295 deficiency in mice results in partially penetrant embryonic lethality and germ cell defects

Lea A. Medeiros[a,b,1], Lucas M. Dennis[a,b,1], Mark E. Gill[a,b,c,1], Hristo Houbaviy[d], Styliani Markoulaki[a], Dongdong Fu[a], Amy C. White[e,2], Oktay Kirak[a], Phillip A. Sharp[b,e], David C. Page[a,b,c], and Rudolf Jaenisch[a,b,3]

[a]Whitehead Institute for Biomedical Research, Cambridge, MA 02139; [b]Department of Biology, Massachusetts Institute of Technology, Cambridge, MA 02139; [c]Howard Hughes Medical Institute and [d]Department of Cell Biology, University of Medicine and Dentistry of New Jersey, Stratford, NJ 08084; and [e]David H. Koch Institute for Integrative Cancer Research, Massachusetts Institute of Technology, Cambridge, MA 02139

Contributed by Rudolf Jaenisch, July 21, 2011 (sent for review January 24, 2011)

Mir-290 through *mir-295* (*mir-290–295*) is a mammalian-specific microRNA (miRNA) cluster that, in mice, is expressed specifically in early embryos and embryonic germ cells. Here, we show that *mir-290–295* plays important roles in embryonic development as indicated by the partially penetrant lethality of mutant embryos. In addition, we show that in surviving *mir-290–295*-deficient embryos, female but not male fertility is compromised. This impairment in fertility arises from a defect in migrating primordial germ cells and occurs equally in male and female mutant animals. Male *mir-290–295*$^{-/-}$ mice, due to the extended proliferative lifespan of their germ cells, are able to recover from this initial germ cell loss and are fertile. Female *mir-290–295*$^{-/-}$ mice are unable to recover and are sterile, due to premature ovarian failure.

In the mouse, miRNA-mediated posttranscriptional regulation is required for normal embryogenesis (1–3) and embryonic germ cell development (4). Whereas critical roles for miRNA biogenesis in early embryos and embryonic germ cells have been established, the role of individual miRNAs in the development of these cell types remains unclear. Six miRNA families comprise the majority of miRNA species cloned from mouse embryonic stem (ES) cells, with miRNAs from the *mir-290* cluster, *mir-290* through *mir-295* (*mir-290–295*), being the most abundant (5). Members of this cluster are the first embryonic miRNAs up-regulated in the zygote (6). It has previously been shown that the *mir-290* cluster miRNAs are processed from a single primary transcript (7) and possess highly similar pre-miRNA sequences (8).

Several studies have addressed the role of *mir-290–295* in embryonic stem (ES) cells where this cluster is a direct target of the *Oct4*, *Sox2*, and *Nanog* regulatory network (9). The *mir-290* cluster is correlated with developmental potency. *Mir-290–295* expression decreases as ES cells differentiate (8). Furthermore, certain members of the miR-290 family were found to increase the efficiency of reprogramming by *Oct4*, *Sox2*, and *Klf4* ~10 fold (10). In addition, members of the miR-290 family promote the G1–S transition and thereby the rapid proliferation characteristic of ES cells (11). The *mir-290* cluster was also implicated in indirect control of de novo DNA methylation in ES cells (12, 13). Taken together, these data imply important roles for *mir-290–295* in ES cells and by extension, early mouse development. In this study, we examined the in vivo consequences of targeted disruption of *mir-290–295* in the developing mouse.

Results

***mir-290–295* Is Specifically Expressed in the Early Embryo and Embryonic Germ Cells.** We have shown that *mir-290–295* is expressed in ES cells and not in adult somatic tissues (8). To address the timing of *mir-290* cluster expression, we performed RT-PCR for the *mir-290–295* primary transcript (*pri-mir-290–295*) throughout early embryonic development on pools of embryos. We observed onset of expression of the primary transcript at the 4–8 cell stage (Fig. 1*A*), consistent with the finding that expression of these miRNAs is up-regulated postzygotically (6). Expression of the *mir-290–295* primary transcript decreased after embryonic day 6.5 (E6.5).

To more closely examine the expression of the *mir-290* cluster miRNAs after gastrulation, we performed RT-PCR for the primary transcript on a panel of embryonic tissues from E14.5 embryos. Expression of *mir-290–295* was detectable in the embryonic testis but not in any other tissue examined (Fig. 1*B*). Because *mir-290–295* has been shown to be expressed in primordial germ cells (4) we analyzed *mir-290* cluster expression in germ cells during embryonic development. Expression of the *mir-290* cluster was observed in gonads of both sexes at E12.5. The primary *mir-290–295* transcript was down-regulated in female gonads between E13.5 and E14.5, whereas in male gonads expression persisted through E14.5 and became undetectable by E15.5 (Fig. 1*C*).

Because the embryonic gonad is composed of both somatic and germ cell populations, we examined *mir-290–295* expression in E14.5 W^v/W^v gonads to test whether *mir-290–295* expression in the E14.5 testis was dependent upon the presence of germ cells. W^v homozygotes harbor a mutation in the *c-kit* gene that impairs primordial germ cell (PGC) migration to the gonad, resulting in loss of germ cells before E14.5 (14). The primary *mir-290–295* transcript was undetectable in embryonic W^v/W^v testes, suggesting that *mir-290–295* expression in embryonic gonads is restricted to the germ cells (Fig. 1*D*).

Generation of *mir-290–295* Mutant Mice. To determine the function of *mir-290–295* in vivo, we generated mice deficient for the 2-kb locus containing these miRNAs by targeted disruption in ES cells (Fig. 2*A*). Two independent *mir-290–295*$^{+/-}$ ES cell lines, where correct targeting had been validated by Southern blot and PCR, were injected into B6DF2 host blastocysts to produce chimeras. Transmission of the targeted allele through the male germline was confirmed by Southern blotting and PCR analysis (Fig. 2*B*). To verify that deletion of the *mir-290–295* locus eliminated expression of the miR-290 family of miRNAs, *mir-290–295* homozygous knockout ES cells lines were produced. Northern blot (Fig. 2*C*) and real-time RT-PCR (data not shown) using probes to detect mature miR-290 family miRNAs failed to detect any of these miRNAs in mutant (*mir-290–295*$^{-/-}$) ES cells, confirming that the targeted deletion resulted in a null allele. These findings suggest that *mir-290–295* is dispensable for maintaining the pluripotent state in embryonic stem cells.

Author contributions: L.A.M., L.M.D., M.E.G., H.H., S.M., P.A.S., D.C.P., and R.J. designed research; L.A.M., L.M.D., M.E.G., H.H., S.M., D.F., A.C.W., and O.K. performed research; L.A.M., L.M.D., M.E.G., H.H., S.M., and O.K. contributed new reagents/analytic tools; L.A.M., L.M.D., M.E.G., and S.M. analyzed data; and L.A.M., L.M.D., M.E.G., and R.J. wrote the paper.

The authors declare no conflict of interest.

[1]L.A.M., L.M.D., and M.E.G. contributed equally to this work.

[2]Present address: Alnylam Pharmaceuticals, Cambridge, MA 02142.

[3]To whom correspondence should be addressed. E-mail: jaenisch@wi.mit.edu.

This article contains supporting information online at www.pnas.org/lookup/suppl/doi:10.1073/pnas.1111241108/-/DCSupplemental.

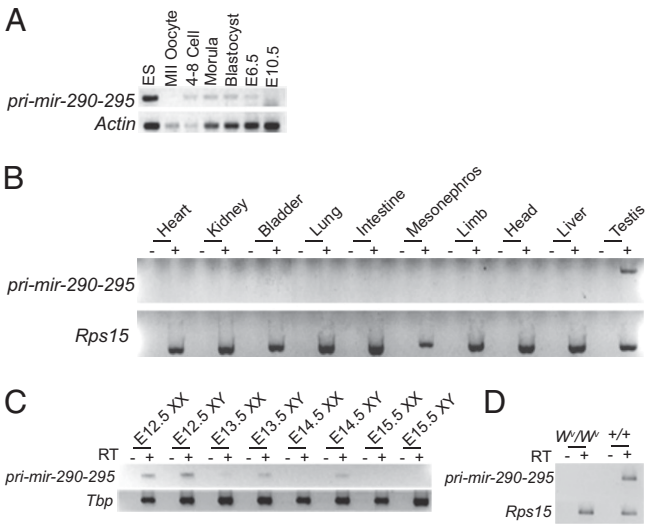

Fig. 1. *mir-290–295* is expressed in the early embryo and in germ cells. (*A*) RT-PCR of primary *mir-290–295* transcript and *Actin* control in early embryos. (*B*) RT-PCR of *mir-290–295* and *Rps15* control in a tissue panel from E14.5 embryos. (*C*) RT-PCR of *mir-290–295* and *Tbp* control in E12.5–E15.5 embryonic gonads from males and females. (*D*) RT-PCR of *mir-290–295* and *Rps15* control in E14.5 testis isolated from wild-type and homozygous *c-kit* (W^v) mutants.

***mir-290–295* Deficiency Results in Partially Penetrant Embryonic Lethality.** *mir-290–295*$^{+/-}$ mice were fertile and indistinguishable from wild-type littermates. When heterozygous animals were intercrossed, we observed a significantly lower fraction of *mir-290–295*$^{-/-}$ offspring than the 25% predicted by Mendelian segregation (Table 1). Only 7% (32 of 452, $P < 0.001$, χ^2) of 4-wk-old postnatal progeny from *mir-290–295*$^{+/-}$ intercrosses were *mir-290–295*$^{-/-}$, suggesting that about three-quarters of the homozygous knockout animals were lost during development. At E18.5, just before birth, the percentage of *mir-290–295*$^{-/-}$ embryos observed (7%, 3 out of 46, $P < 0.01$, χ^2) was identical to that seen at postnatal stages, indicating that perinatal lethality was not responsible for the loss of *mir-290–295*$^{-/-}$ embryos (Table 1).

To determine when during gestation *mir-290–295*$^{-/-}$ embryos were lost, embryos from heterozygous intercrosses were isolated at blastocyst (E3.5) and mid-late gestation (E8.5–E18.5) stages of development. Mutant (*mir-290–295*$^{-/-}$) blastocysts appeared morphologically indistinguishable from their wild-type and heterozygous counterparts and were observed at the predicted Mendelian ratio of 25% (32 out of 117 total blastocysts). Further analysis of embryos at mid-late gestation suggested that *mir-290–295*$^{-/-}$ embryos were lost over a period between E11.5 and E18.5.

Even though mutant embryos were observed at the predicted Mendelian ratio at E8.5, E9.5, E10.5, E11.5, and E13.5, ~50–60% of these embryos (Table 2) displayed abnormalities not observed in their wild-type or heterozygous littermates. Two abnormal phenotypes were observed. Before E10.5, about 16% of the mutant embryos were partially or completely localized outside the yolk sac (Fig. 3). Such abnormal embryos were not observed at later stages presumably because they had died and been reabsorbed.

The second abnormal phenotype, comprising about 40% of the mutant embryos, showed general developmental delays as early as E8.5. These mutants had fewer somites than their wild-type or heterozygous littermates and showed delays in chorioallantoic attachment, axial turning, and neural tube closure.

Table 1. *mir-290–295* deficiency results in partially penetrant embryonic lethality

	Wild-type: het: knockout (%)	Reabsorbed embryos
E3.5	29: 56: 32 (27)	—
E7.5	2: 4: 2 (25)	0
E8.5	7: 21: 13 (32)	0
E9.5	18: 30: 21 (30)	0
E10.5	14: 36: 12 (19)	1
E11.5	10: 19: 6 (17)	4
E13.5	16: 26: 10 (19)	10
E18.5	8: 35: 3 (7)*	8
Postnatal (4 wk)	168: 252: 32 (7)†	—

Embryos from heterozygous matings were dissected at the specified timepoints and genotyped. Reabsorbed embryos refer to embryos that were too disintegrated to separate from the maternal tissue and were therefore not genotyped.
*$P < 0.01$, χ^2 test.
†$P < 0.001$, χ^2 test.

Adult *mir-290–295*$^{-/-}$ Females Are Sterile, Whereas Adult *mir-290–295*$^{-/-}$ Males Are Fertile. Surviving *mir-290–295*$^{-/-}$ animals were healthy and phenotypically normal, although homozygous knockout females were infertile. Ovaries from adult (5–12 wk postpartum) *mir-290–295*$^{-/-}$ animals were small, having a volume less than 20% that of wild-type littermates (Fig. 4*A*). Ovaries from homozygous knockouts older than 10 wk contained no observable

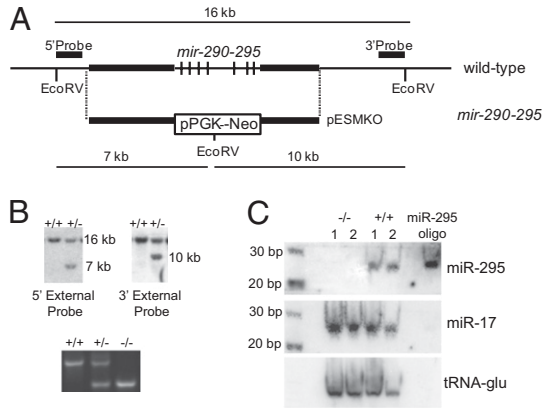

Fig. 2. Targeted disruption of the *mir-290–295* locus. (*A*) Targeting strategy for generation of the *mir-290–295* allele. (*B*) Southern blot and PCR confirmation of correct targeting of the *mir-290–295* locus. (*C*) Northern blot validation of *mir-290–295* targeting.

Table 2. *mir-290–295*-deficient embryos display defects at midgestation stages

	Total number of *mir-290–295*$^{-/-}$ embryos observed	Number of abnormal or reabsorbed *mir-290–295*$^{-/-}$ observed (%)
E3.5	32	0 (0)
E8.5	25	16 (64)
E9.5	39	26 (66)
E10.5	22	14 (64)
E11.5	10	5 (50)
E13.5	21	11 (52)
E18.5	11	8 (73)

mir-290–295$^{-/-}$ embryos analyzed in this table are progeny from both *mir-290–295*$^{+/-}$ intercrosses and *mir-290–295*$^{+/-}$ × *mir-290–295*$^{-/-}$ crosses. "Abnormal" refers to embryos that were either observed outside the yolk sac or were developmentally delayed compared with wild-type littermates.

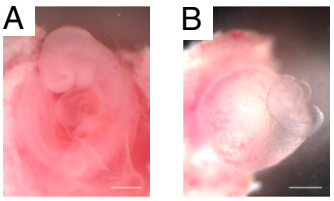

Fig. 3. Some *mir-290–295*$^{-/-}$ embryos were observed outside the yolk sac. (*A*) Wild-type E9.5 embryo. (*B*) *mir-290–295*$^{-/-}$ E9.5 embryo located outside of the yolk sac. (Scale bars, 500 μM.)

follicular structures (data not shown). In the ovaries of 5- to 8-wk-old *mir-290–295*$^{-/-}$ animals, small numbers of follicles were occasionally observed (Fig. 4 *C* and *E*).

Whereas testes from adult *mir-290–295*$^{-/-}$ males were relatively similar in size to the testes of wild-type males (Fig. 4*F*), histological periodic acid-Schiff (PAS)–stained sections of *mir-290–295*$^{-/-}$ males showed empty seminiferous tubules (black rectangle in Fig. 4*H*) alongside tubules filled with germ cells at various stages of spermatogenesis (Fig. 4 *H* and *J*). *Mir-290–295*$^{-/-}$ males regularly fathered litters with both wild-type and *mir-290–295*$^{+/-}$ females and can therefore be considered fertile.

Both Male and Female *mir-290–295*$^{-/-}$ Early Postnatal Gonads Show Reduced Germ Cell Numbers. Examination of ovaries and testes from postnatal day 5 (P5) animals revealed a reduced number of gonocytes in both males and females. At P5, *mir-290–295*$^{-/-}$ ovaries contained less than 20% as many oocytes as wild-type ovaries, as determined by histological analysis and immunostaining for mouse vasa homolog (MVH), a germ cell marker (15) (Fig. S1 *A–D*). In contrast to wild-type ovaries (Fig. S1 *A* and *C*), *mir-290–295*$^{-/-}$ ovaries displayed very few primordial follicles (Fig. S1 *B* and *D*). Consistent with these data, P10 *mir-290–295*$^{-/-}$ ovaries showed severe depletion of the primordial follicle pool (Fig. S1 *F* and *H* compared with Fig. S1 *E* and *G*). Because the primordial follicle pool is a finite population (16), once all of the follicles have been recruited from the pool for maturation and/or death, the female will no longer be fertile.

Mir-290–295$^{-/-}$ testes also showed fewer germ cells than controls at P5 (Fig S1 *I–L*). Chains of 3–4 gonocytes were observed in P5 homozygous knockout males, suggesting that the male *mir-290–295*$^{-/-}$ germ cells were still proliferating. Furthermore, at P10, tubules in the homozygous knockout male contained more than the clusters of three to four gonocytes observed at P5, further suggesting that the male *mir-290–295*$^{-/-}$ germ cells continued to proliferate (Fig. S1 *M–P*). These data are not surprising, considering that the expression data in Fig. 1*C* indicated that the *mir-290* cluster is not expressed after E14.5 in males.

The above data, combined with the observation of empty seminiferous tubules in the adult male homozygous knockout (Fig. 4 *H* and *J*), suggest that the original germ cell defect is initially sex neutral and that males are able to regain fertility by clonal expansion of surviving germ cells.

Both Male and Female *mir-290–295*$^{-/-}$ Embryonic Gonads Show Germ Cell Depletion. We sought to determine the timepoint during development when a difference in germ cell number or localization became apparent between homozygous knockouts and their wild-type siblings. Because *mir-290–295* expression becomes undetectable after E13.5 in females and E14.5 in males (Fig. 1*C*), we examined E13.5 gonads by immunostaining for the germ cell marker MVH. Inspection of *mir-290–295*$^{-/-}$ ovaries and testes at E13.5 revealed a dramatic reduction in the number of MVH^{+} cells relative to control embryonic gonads (Fig. 5 *A–E*). To ensure that the loss of MVH expression was indicative of decreased germ cell number, and not a gene-specific effect of *mir-290–295* deficiency, we examined expression of another germ cell marker, germ cell nuclear antigen (GCNA) (17) in E13.5 homozygous knockout gonads and found a similar reduction in the number of GCNA^{+} cells (data not shown).

We then examined E11.5 embryos to determine whether reduced numbers of *mir-290–295*$^{-/-}$ PGCs were colonizing the

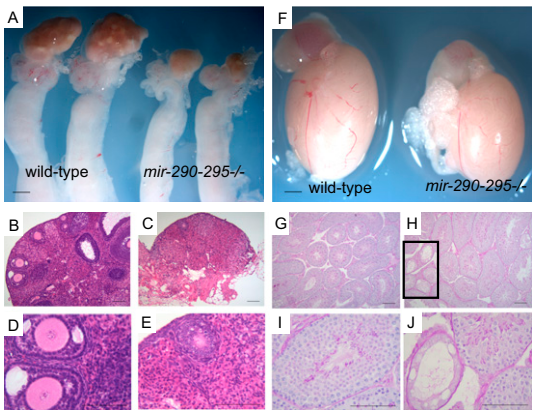

Fig. 4. Adult male *mir-290–295*$^{-/-}$ testes show reduced germ cells compared with wild-type testes, whereas adult female *mir-290–295*$^{-/-}$ ovaries are atrophied. (*A*) Ovaries and reproductive tracts from 8-wk-old wild-type and *mir-290–295*$^{-/-}$ females. (Scale bar, 1 mm.) (*B–E*) Hematoxylin and eosin-stained ovary sections from adult wild-type (*B* and *D*) and *mir-290–295*$^{-/-}$ (*C* and *E*) animals. (Scale bars, 100 μM.) (*F*) Testes from 8-wk-old wild-type and *mir-290–295*$^{-/-}$ males. Note that the smaller testes size of the knockout male is at least partially due to the smaller body weight of the knockout animal. (Scale bar, 1 mm.) (*G–J*) Periodic acid-Schiff (PAS)–stained testes sections from adult wild-type (*G* and *I*) and *mir-290–295*$^{-/-}$ (*H* and *J*) males. Black rectangle in *H* highlights area with empty seminiferous tubules. (Scale bars, 100 μM.)

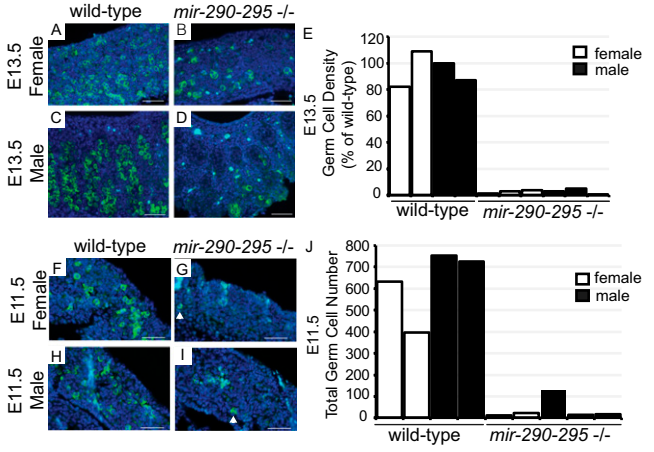

Fig. 5. Both male and female *mir-290–295*$^{-/-}$ embryonic gonads show reduced germ cell numbers as early as E11.5. (*A–D*) MVH immunostaining of sections of E13.5 ovaries (*A* and *B*) and testes (*C* and *D*) from wild-type (*A* and *C*) and *mir-290–295*$^{-/-}$ (*B* and *D*) embryos. (Scale bars, 50 μM.) (*E*) Germ cell density (germ cells/area of gonadal section for ovaries and germ cells/testis cord area for testes) as determined by MVH staining. Each bar represents a single embryo with black bars indicating male embryos and white bars, female embryos. (*F–I*) MVH immunostaining of E11.5 embryo sections from wild-type (*F* and *H*) and *mir-290–295*$^{-/-}$ (*G* and *I*) embryos. (Scale bars, 50 μM.) White arrows point to germ cells in *G* and *I*. The additional green cells in *I* are blood cells. (*J*) Total germ cell numbers in E11.5 gonads as determined by serial sectioning and MVH staining. Each bar represents a single embryo with black bars indicating male embryos and white bars, female embryos.

genital ridges. At E11.5, most male and female *mir-290–295*$^{-/-}$ genital ridges exhibited less than 5% as many germ cells as found in wild-type littermate controls (Fig. 5 *F–J*), as determined by MVH immunostaining.

***mir-290–295*$^{-/-}$ Animals Show Many Mislocalized Primordial Germ Cells.** On the basis of the reduced number of germ cells colonizing the genital ridges in E11.5 mutants and the fact that *mir-290–295* is expressed in migrating primordial germ cells (4) we explored the possibility that mutant embryos exhibited defective germ cell migration. PGCs in the developing mouse embryo migrate from their origin in the proximal epiblast, through the developing hindgut, to the genital ridges (18, 19). We used two different germ cell markers, alkaline phosphatase (AP) (20) and *Oct4*, to locate germ cells in the midgestation embryo. Alkaline phosphatase expression was detected by whole-mount staining, whereas an *Oct4-GFP* transgene was used to monitor *Oct4* expression (21). In wild-type animals at E9.5, PGCs were located almost exclusively in the hindgut and dorsal mesentery (Fig. 6 *A*, *C*, and *D*). Although there was great variability among PGC numbers, both *mir-290–295*$^{-/-}$ males and females had about one-fourth as many germ cells in the hindgut and mesentery as wild-type animals of the same developmental stage (Fig. 6 *B–D*).

Surprisingly, mutant males and females exhibited AP$^+$ *Oct4*$^+$ cells on the ventral surface of the embryo near the hindlimb buds and the base of the tail (Fig. 6*B*). On average, mutant embryos had 40 of these ectopic PGCs, whereas their wild-type counterparts had 10 or fewer (Fig. 6*D*). These ectopic PGCs were observed as late as E11.5 (data not shown). A difference between germ cell localization in mutants and control littermates could be observed as early as E8.5. In *Oct4-GFP* wild-type embryos at the 7-somite stage, *Oct4*$^+$ cells had already moved into the hindgut (Fig. S2*A*). In contrast, *Oct4*$^+$ cells in the 7-somite stage *Oct4-GFP mir-290–295*$^{-/-}$ embryos were clustered together at the base of the allantois (Fig. S2 *B* and *C*). Taken together, these data suggest that loss of germ cells in *mir-290–295*$^{-/-}$ animals is at least partially due to improper germ cell migration.

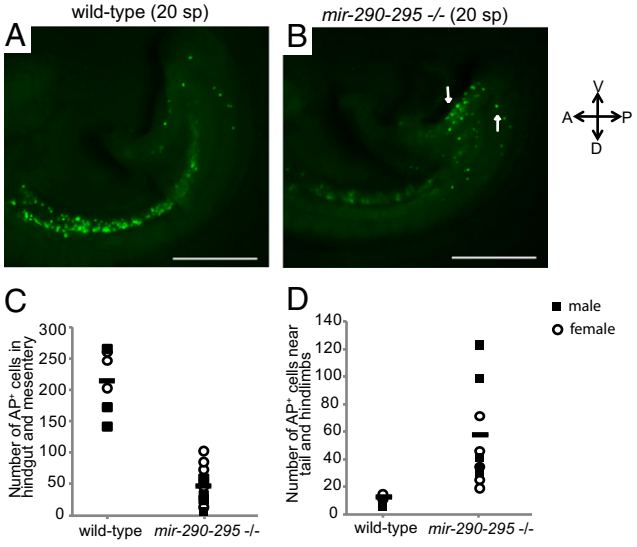

Fig. 6. Primordial germ cells (PGCs) are mislocalized in *mir-290–295*$^{-/-}$ embryos. (*A* and *B*) Images of E9.5 *Oct4-GFP* wild-type (*A*) and *Oct4-GFP mir-290–295*$^{-/-}$ (*B*) embryos. (Scale bars, 1 mm.) The numbers in parentheses refer to the number of somite pairs in each embryo. Arrows point to PGCs located near the tail. (*C*) Number of PGCs, as determined by alkaline phosphatase staining, in the hindgut and mesentery of E9.5 embryos. Black bars indicate the average number of PGCs for each genotype. (*D*) Number of PGCs, as determined by alkaline phosphatase staining, near the hindlimb and base of tail, in E9.5 embryos. Black bars indicate the average number of PGCs for each genotype.

***mir-290–295*$^{-/-}$ Germ Cells Do Not Undergo Premature Cell Cycle Arrest or Apoptosis.** Because the *mir-290* cluster has been shown to regulate the G1–S transition (11), and protect against apoptosis in ES cells (22), we explored the possibility that *mir-290–295*$^{-/-}$ germ cells might have undergone apoptosis or premature cell cycle arrest. We studied two timepoints during germ cell development: E9.5, when germ cells are migrating toward the developing gonad and E12.5, after germ cells have arrived in the gonad but before they have undergone mitotic arrest (in males) or meiotic arrest (in females). E9.5 embryos were serially sectioned and stained for either K_i-67 or cleaved caspase-3. In all sections, SSEA-1 was used to identify the migrating PGCs (23). At least 90% of both wild-type and *mir-290–295*$^{-/-}$ migrating PGCs were K_i-67$^+$ (Fig. S3 *A–G*). K_i-67 protein is expressed in all proliferating cells during the late G_1, S, G_2, and M phases of the cell cycle. Only cells in the G_0 phase of the cell cycle do not express K_i-67 (24, 25). Therefore, the data from E9.5 animals indicate that *mir-290–295*$^{-/-}$ PGCs are actively cycling. Furthermore, neither wild-type nor *mir-290–295*$^{-/-}$ E9.5 PGCs were cleaved caspase-3$^+$ (Fig. S3 *H–O*), indicating that *mir-290–295*$^{-/-}$ PGCs are not undergoing apoptosis. This is consistent with previous reports that germ cell apoptosis is mediated by the caspase-3 pathway (26).

Similar results were obtained with E12.5 gonocytes. Male and female wild-type and *mir-290–295*$^{-/-}$ E12.5 gonads were serially sectioned and stained for either MVH and proliferating cell nuclear antigen (PCNA) or SSEA-1 and cleaved caspase-3. PCNA, like K_i-67, is a marker of actively cycling cells (27). (Because double K_i-67 and MVH immunostaining proved difficult, PCNA was substituted for K_i-67.) At E12.5, in both male and female gonads, at least 85% of the gonocytes were PCNA$^+$, and therefore actively cycling (Fig. S4). In addition, neither wild-type nor *mir-290–295*$^{-/-}$ males or females exhibited any cleaved caspase-3$^+$ germ cells (Fig. S5). Taken together these data show that decreased numbers of germ cells in the *mir-290–295*$^{-/-}$ animal cannot be explained by apoptosis or failure of the mutant germ cells to proliferate.

Discussion

In this study, we investigated the biological function of the *mir-290* cluster by targeted deletion in the mouse. Although miRNAs of the *mir-290* cluster are the first miRNAs up-regulated in the developing embryo, this cluster was not required for preimplantation development or ES cell pluripotency. Instead, we found that *mir-290–295* deficiency had a significant effect between implantation and midgestation and during germ cell development. Approximately three-quarters of *mir-290–295*-deficient embryos were lost during embryonic development. The surviving quarter of homozygous knockouts showed a germ cell loss. Adult male mutants recover from this loss, whereas female mutants do not and are sterile.

***mir-290–295* Deficiency Confers an Incompletely Penetrant Embryonic Lethality.** The earliest abnormality in *mir-290–295*$^{-/-}$ animals was observed at E8.5. Specifically, about 16% of *mir-290–295*-deficient embryos at E8.5 (and E9.5 and E10.5) were found either partially or completely outside of the yolk sac. The phenomenon of postimplantation embryos located either partially or completely outside the yolk sac has been observed for mutants of several genes involved in patterning the embryo during gastrulation. These mutants include the *Type II Activin* receptor knockout (28), *Hnf3β* knockout (29), *Otx2* knockout (30), *Lpp3* knockout (31), *Axin* knockout (32), and *Nodal* hypomorph (33). The exact mechanism by which these embryos end up outside the yolk sac remains unclear (29, 34).

One intriguing possibility is that the *mir-290–295* cluster might play a role in embryonic patterning by regulating *lefty1*. Both *lefty1*

and *lefty2* have been shown to be targets of the miR-290 family miRNAs (9, 12). In zebrafish, miR-430, which has the same AAGUGC seed sequence as many of the miRNAs in the *mir-290* cluster, balances the expression of the *Nodal* agonist *squint* and the TGF-β *Nodal* antagonist *lefty* (35). In human ES cells, depletion of miR-302, which targets *lefty1* and *lefty2*, leads to a strong decrease in the expression of mesodermal and endodermal markers (36). The *mir-290–295* mutant mouse would provide a unique opportunity to test the hypothesis that AAGUGC seed miRNAs are involved in balancing *lefty-Nodal* signaling.

***mir-290–295* Deficiency Results in Germ Cell Loss.** Approximately 25% of *mir-290–295*$^{-/-}$ animals survived to adulthood. Although adult female homozygous knockouts were sterile and male homozygous knockouts were fertile, the germ cell loss leading to sterility in the female was first observed in both sexes at E11.5. This suggests that fewer germ cells were colonizing the gonads in both *mir-290–295*$^{-/-}$ females and males. Observations of migrating PGCs revealed a reduction in the number of correctly localized germ cells in *mir-290–295*-deficient animals. In E9.5 male and female mutants, the decreased number of PGCs properly localized to the hindgut area correlated with the increased number of ectopic germ cells observed on the ventral posterior surface of the embryo. These data suggest that the germ cell loss observed in the mutant is due to mislocalization of a subpopulation of primordial germ cells, which are subsequently unable to colonize the gonad and therefore cannot contribute to the germ cell pool.

Given that members of the *mir-290–295* family have been shown to regulate the G1–S transition (11), and recently apoptosis (22), in ES cells, we investigated whether increased apoptosis or a block in proliferation could explain the germ cell loss in the mutant animals. No cleaved caspase-3^{+} PGCs were observed in wild-type or *mir-290–295*$^{-/-}$ germ cells at E9.5 or E12.5. In E9.5 and E12.5 animals, at least 85% of migrating PGCs in both wild-type and *mir-290–295*$^{-/-}$ animals were actively cycling. Whereas the above results rule out the possibility of premature cell cycle arrest in *mir-290–295*$^{-/-}$ PGCs, they cannot exclude the possibility that slower proliferation kinetics of the mutant germ cells contributes to the decrease in germ cells caused by mislocalization.

Nevertheless, whereas a defective G1–S transition might be able to explain part of the germ cell loss realized at E11.5 and E13.5, it would not explain the primary observation that some *mir-290–295*$^{-/-}$ germ cells are mislocalized during migration. Ectopic PGCs localized in or near the tail have been previously reported in mice deficient for the proapoptotic protein Bax (26, 37, 38). Although the majority of ectopic PGCs in *Bax*$^{-/-}$ mice were found within the abdominal midline dorsal body wall, some ectopic PGCs were also observed on the tail. Unlike *Bax*$^{-/-}$ embryos, *mir-290–295*$^{-/-}$ embryos do not display ectopic germ cells in or near the abdominal midline body wall, suggesting that mislocalization of *mir-290–295*$^{-/-}$ germ cells is not simply a consequence of faulty apoptotic pathways.

Ectopic "tail" PGCs are hypothesized to arise from PGCs, which fail to become incorporated into the hindgut during the initial stages of germ cell migration (37). Our observations are consistent with this model. At E8.5, although wild-type PGCs have already entered the developing hindgut, the majority of mutant PGCs have not yet started to migrate and instead are stuck near the base of the allantois (Fig. S2). Whether the failure of germ cells to disperse by E8.5 is due to cell autonomous defects within the germ cells or defects in the surrounding soma still remains unclear. Recently, miR-430, which has the same seed sequence as many members of the *mir-290–295* cluster, was implicated in PGC migration in the zebrafish (39). Interestingly, loss of miR-430 led to defective migration due to misexpression of chemokines in the surrounding soma. The *mir-290–295* locus is expressed in migrating PGCs (4). Furthermore, the *mir-290–295* primary transcript is expressed in the early (E6.5) embryo and its expression decreases by E10.5 (Fig. 1*A*). Currently it is not known whether or not miR-290 miRNAs are present in the tissues through which PGCs must migrate. Therefore, we cannot rule out the possibility that a subtle defect in the surrounding soma might be the cause of the ectopic germ cells.

Little is known about the genes involved (both in the germ cells themselves and the soma) in the early stages (E7.5–E8.5) of germ cell migration. Although, on the basis of misexpression studies, *fragilis* was thought to play a role in movement of the primordial germ cells from the epiblast into the endoderm (40), a *fragilis* knockout showed no defects in germ cell localization (41). To the best of our knowledge, the *mir-290–295* deletion represents the first germ cell mutant where PGCs mislocalize to the ventral surface of the embryo near the developing hindlimbs. Thus, it will be of interest to understand the molecular mechanisms of how the *mir-290–295* cluster is involved in the early stages of germ cell migration.

Our data cannot exclude the possibility that the migration defect observed is an indirect effect of improper germ cell specification. We do not know whether the same number of germ cells are allocated in *mir-290–295*$^{-/-}$ animals and wild-type animals. Further experiments beyond the scope of this work are required to address these questions.

The ability of the *mir-290–295*$^{-/-}$ males to recover from the early germ cell loss is likely a result of the extended proliferative lifespan of male germ cells rather than a direct consequence of *mir-290–295* deficiency. Recovery of male germ cells after embryonic sex-neutral depletion has been previously reported (42, 43) and is therefore not unique to the *mir-290–295*$^{-/-}$. Male germ cells undergo mitotic arrest around E13.5 but then resume mitosis a few days after birth (43). In contrast, female germ cells enter meiosis around E13.5, thereby establishing the total oocyte pool for adult life (16). The extra proliferative time in the males allows for additional clonal expansion of the few surviving *mir-290–295*$^{-/-}$ gonocytes, which results in enough germ cells for the *mir-290–295*$^{-/-}$ males to maintain fertility.

***mir-290–295* Deficiency Confers Incompletely Penetrant Phenotypes.** The phenotypes conferred by *mir-290–295* deficiency are characterized by variable expressivity and incomplete penetrance. The mixed background of the mice used in this study (129/C57BL6) may contribute to the incomplete penetrance of the embryonic lethality. However, given what is known about miRNAs, the partially penetrant embryonic lethality might also be explained by the function of the *mir-290* cluster itself. MiRNAs have been shown to confer robustness to developmental systems (44–48). It was recently shown that random fluctuations in gene expression can result in an incompletely penetrant phenotype when a certain level of gene expression is required to pass a threshold to cause an outcome (49). Consistent with this, deletions of various miRNAs have been shown to confer partially penetrant phenotypes (50–53). Taken together, these data lead us to speculate that the loss of *mir-290–295* expression might cause fluctuations in gene expression patterns. Those mutants with gene expression patterns that differ greatly from wild-type would not survive, whereas mutants with gene expression patterns close to their wild-type counterparts would be able to develop normally during this period. Presumably after this time window, the role of *mir-290–295* becomes less critical. Therefore, any mutants surviving this time period also survive to adulthood.

Materials and Methods

RT-PCR. RNA samples were isolated by homogenizing tissue or cells in TRIzol (Invitrogen) following the manufacturer's suggested protocol. Five micrograms of total RNA was DNase I treated using the DNA-Free RNA kit (Zymo Research). One microgram of DNase I-treated RNA was reverse transcribed using a First Strand Synthesis kit (Invitrogen). PCR was performed using 1/80 of the reverse transcription reaction. The following primer sequences were used to determine *pri-mir-290–295* expression: 5′-GAACCTCACGGGAAGTGACC-3′ (forward primer) and 5′-TGCCCACAGGAGAGACTCAA-3′ (reverse primer).

Northern Blot Analysis. RNA was extracted using TRIzol (Invitrogen) following the manufacturer's instructions. A total of 30 μg of total RNA was electrophoresed for 45 min at 35 W, and semidry transferred to Hybond-NX nylon membrane (Amersham Biosciences) at 18 V for 1.5 h at 4 °C. RNA was cross-linked and incubated with locked nucleic acid (LNA) probe as previously described (54, 55). After washing, membranes were exposed to a phosphorimager screen for 1–3 d, depending on the probe. Probes were synthesized by IDT: (*i*) miR-17, C+TAC+CTG+CAC+TGT+AAG+CAC+TTT+G; (*ii*) miR-295, A+GAC+TCA+AAA+GTA+GTA+GCA+CTT+T; and (*iii*) tRNA glu, TGGAGGTTCCAC-CGAGAT, where + indicates that the following nucleotide is an LNA.

Generation of *mir-290–295*$^{-/-}$ Mice. Mice deficient for *mir-290–295* were generated by targeted disruption of the endogenous *mir-290–295* locus via homologous recombination in ES cells. Upstream and downstream arms were PCR amplified from RPCI-23–222D1 BAC DNA, resulting in a construct where 2.1 kb of the *mir-290–295* locus (including the mature miRNA sequences) was replaced by a 1.6-kb neomycin resistance selection cassette (Fig. 2*A*). This targeting construct was electroporated into V6.5 ES cells that were then subjected to selection with G418. After 10 d of selection, G418 resistant clones were analyzed by Southern blotting with external probes. Clones exhibiting correct targeting were injected into B6D2F2 recipient blastocysts for subsequent chimera generation. For this study, mice were maintained on a 129Sv/J × C57BL/6 mixed genetic background. The committee on animal care at the Massachusetts Institute of Technology approved all experiments involving mice.

ACKNOWLEDGMENTS. We thank Jessica Dausman and Ruth Flannery for technical assistance with the generation of chimeras and animal husbandry; George Enders for GCNA antisera; and members of the R.J., D.C.P., and P.A.C. laboratories for critical discussions. This work was supported by National Institutes of Health Grants 5-F32-HD051190 (to A.C.W.), RO1-GM34277 (to P.A.S.), and 5R37CA084198 and 5R01-HD045022 (to R.J), National Cancer Institute Grant PO1-CA42063 (to P.A.S.) and Core Grant P30-CA14051 (to Koch Institute), and the Howard Hughes Medical Institute (D.C.P.).

1. Bernstein E, et al. (2003) Dicer is essential for mouse development. *Nat Genet* 35: 215–217.
2. Liu J, et al. (2004) Argonaute2 is the catalytic engine of mammalian RNAi. *Science* 305: 1437–1441.
3. Wang Y, Medvid R, Melton C, Jaenisch R, Blelloch R (2007) DGCR8 is essential for microRNA biogenesis and silencing of embryonic stem cell self-renewal. *Nat Genet* 39: 380–385.
4. Hayashi K, et al. (2008) MicroRNA biogenesis is required for mouse primordial germ cell development and spermatogenesis. *PLoS One* 3(3):e1738.
5. Calabrese JM, Seila AC, Yeo GW, Sharp PA (2007) RNA sequence analysis defines Dicer's role in mouse embryonic stem cells. *Proc Natl Acad Sci USA* 104:18097–18102.
6. Tang F, et al. (2007) Maternal microRNAs are essential for mouse zygotic development. *Genes Dev* 21:644–648.
7. Houbaviy HB, Dennis L, Jaenisch R, Sharp PA (2005) Characterization of a highly variable eutherian microRNA gene. *RNA* 11:1245–1257.
8. Houbaviy HB, Murray MF, Sharp PA (2003) Embryonic stem cell-specific MicroRNAs. *Dev Cell* 5:351–358.
9. Marson A, et al. (2008) Connecting microRNA genes to the core transcriptional regulatory circuitry of embryonic stem cells. *Cell* 134:521–533.
10. Judson RL, Babiarz JE, Venere M, Blelloch R (2009) Embryonic stem cell-specific microRNAs promote induced pluripotency. *Nat Biotechnol* 27:459–461.
11. Wang Y, et al. (2008) Embryonic stem cell-specific microRNAs regulate the G1-S transition and promote rapid proliferation. *Nat Genet* 40:1478–1483.
12. Sinkkonen L, et al. (2008) MicroRNAs control de novo DNA methylation through regulation of transcriptional repressors in mouse embryonic stem cells. *Nat Struct Mol Biol* 15:259–267.
13. Benetti R, et al. (2008) A mammalian microRNA cluster controls DNA methylation and telomere recombination via Rbl2-dependent regulation of DNA methyltransferases. *Nat Struct Mol Biol* 15:998.
14. Nocka K, et al. (1990) Molecular bases of dominant negative and loss of function mutations at the murine c-kit/white spotting locus: W37, Wv, W41 and W. *EMBO J* 9:1805–1813.
15. Fujiwara Y, et al. (1994) Isolation of a DEAD-family protein gene that encodes a murine homolog of Drosophila vasa and its specific expression in germ cell lineage. *Proc Natl Acad Sci USA* 91:12258–12262.
16. Bristol-Gould SK, et al. (2006) Fate of the initial follicle pool: Empirical and mathematical evidence supporting its sufficiency for adult fertility. *Dev Biol* 298:149–154.
17. Enders GC, May JJ, 2nd (1994) Developmentally regulated expression of a mouse germ cell nuclear antigen examined from embryonic day 11 to adult in male and female mice. *Dev Biol* 163:331–340.
18. Molyneaux KA, Stallock J, Schaible K, Wylie C (2001) Time-lapse analysis of living mouse germ cell migration. *Dev Biol* 240:488–498.
19. Molyneaux KA, et al. (2003) The chemokine SDF1/CXCL12 and its receptor CXCR4 regulate mouse germ cell migration and survival. *Development* 130:4279–4286.
20. Ginsburg M, Snow MH, McLaren A (1990) Primordial germ cells in the mouse embryo during gastrulation. *Development* 110:521–528.
21. Yeom YI, et al. (1996) Germline regulatory element of Oct-4 specific for the totipotent cycle of embryonal cells. *Development* 122:881–894.
22. Zheng GX, et al. (2011) A latent pro-survival function for the mir-290-295 cluster in mouse embryonic stem cells. *PLoS Genet* 7:e1002054.
23. Fox N, Damjanov I, Martinez-Hernandez A, Knowles BB, Solter D (1981) Immunohistochemical localization of the early embryonic antigen (SSEA-1) in postimplantation mouse embryos and fetal and adult tissues. *Dev Biol* 83:391–398.
24. Scholzen T, Gerdes J (2000) The Ki-67 protein: From the known and the unknown. *J Cell Physiol* 182:311–322.
25. Gerdes J, Schwab U, Lemke H, Stein H (1983) Production of a mouse monoclonal antibody reactive with a human nuclear antigen associated with cell proliferation. *Int J Cancer* 31:13–20.
26. Runyan C, et al. (2006) Steel factor controls midline cell death of primordial germ cells and is essential for their normal proliferation and migration. *Development* 133: 4861–4869.
27. Wrobel KH, Bickel D, Kujat R (1996) Immunohistochemical study of seminiferous epithelium in adult bovine testis using monoclonal antibodies against Ki-67 protein and proliferating cell nuclear antigen (PCNA). *Cell Tissue Res* 283:191–201.
28. Song J, et al. (1999) The type II activin receptors are essential for egg cylinder growth, gastrulation, and rostral head development in mice. *Dev Biol* 213:157–169.
29. Dufort D, Schwartz L, Harpal K, Rossant J (1998) The transcription factor HNF3beta is required in visceral endoderm for normal primitive streak morphogenesis. *Development* 125:3015–3025.
30. Ang SL, et al. (1996) A targeted mouse Otx2 mutation leads to severe defects in gastrulation and formation of axial mesoderm and to deletion of rostral brain. *Development* 122:243–252.
31. Escalante-Alcalde D, et al. (2003) The lipid phosphatase LPP3 regulates extra-embryonic vasculogenesis and axis patterning. *Development* 130:4623–4637.
32. Zeng L, et al. (1997) The mouse Fused locus encodes Axin, an inhibitor of the Wnt signaling pathway that regulates embryonic axis formation. *Cell* 90:181–192.
33. Lowe LA, Yamada S, Kuehn MR (2001) Genetic dissection of nodal function in patterning the mouse embryo. *Development* 128:1831–1843.
34. Foley AC, Stern CD (2001) Evolution of vertebrate forebrain development: How many different mechanisms? *J Anat* 199:35–52.
35. Choi WY, Giraldez AJ, Schier AF (2007) Target protectors reveal dampening and balancing of Nodal agonist and antagonist by miR-430. *Science* 318:271–274.
36. Rosa A, Spagnoli FM, Brivanlou AH (2009) The miR-430/427/302 family controls mesendodermal fate specification via species-specific target selection. *Dev Cell* 16:517–527.
37. Runyan C, Gu Y, Shoemaker A, Looijenga L, Wylie C (2008) The distribution and behavior of extragonadal primordial germ cells in Bax mutant mice suggest a novel origin for sacrococcygeal germ cell tumors. *Int J Dev Biol* 52:333–344.
38. Stallock J, Molyneaux K, Schaible K, Knudson CM, Wylie C (2003) The pro-apoptotic gene Bax is required for the death of ectopic primordial germ cells during their migration in the mouse embryo. *Development* 130:6589–6597.
39. Staton AA, Knaut H, Giraldez AJ (2011) miRNA regulation of Sdf1 chemokine signaling provides genetic robustness to germ cell migration. *Nat Genet* 43:204–211.
40. Tanaka SS, Yamaguchi YL, Tsoi B, Lickert H, Tam PP (2005) IFITM/Mil/fragilis family proteins IFITM1 and IFITM3 play distinct roles in mouse primordial germ cell homing and repulsion. *Dev Cell* 9:745–756.
41. Lange UC, et al. (2008) Normal germ line establishment in mice carrying a deletion of the Ifitm/Fragilis gene family cluster. *Mol Cell Biol* 28:4688–4696.
42. Luoh SW, et al. (1997) Zfx mutation results in small animal size and reduced germ cell number in male and female mice. *Development* 124:2275–2284.
43. Lu B, Bishop CE (2003) Late onset of spermatogenesis and gain of fertility in POG-deficient mice indicate that POG is not necessary for the proliferation of spermatogonia. *Biol Reprod* 69:161–168.
44. Tsang J, Zhu J, van Oudenaarden A (2007) MicroRNA-mediated feedback and feedforward loops are recurrent network motifs in mammals. *Mol Cell* 26:753–767.
45. Hornstein E, Shomron N (2006) Canalization of development by microRNAs. *Nat Genet* 38(Suppl):S20–S24.
46. Herranz H, Cohen SM (2010) MicroRNAs and gene regulatory networks: Managing the impact of noise in biological systems. *Genes Dev* 24:1339–1344.
47. Li X, Cassidy JJ, Reinke CA, Fischboeck S, Carthew RW (2009) A microRNA imparts robustness against environmental fluctuation during development. *Cell* 137:273–282.
48. Martinez NJ, et al. (2008) A C. elegans genome-scale microRNA network contains composite feedback motifs with high flux capacity. *Genes Dev* 22:2535–2549.
49. Raj A, Rifkin SA, Andersen E, van Oudenaarden A (2010) Variability in gene expression underlies incomplete penetrance. *Nature* 463:913–918.
50. Fish JE, et al. (2008) miR-126 regulates angiogenic signaling and vascular integrity. *Dev Cell* 15:272–284.
51. Li Y, Wang F, Lee JA, Gao FB (2006) MicroRNA-9a ensures the precise specification of sensory organ precursors in Drosophila. *Genes Dev* 20:2793–2805.
52. Kuhnert F, et al. (2008) Attribution of vascular phenotypes of the murine Egfl7 locus to the microRNA miR-126. *Development* 135:3989–3993.
53. Zhao Y, et al. (2007) Dysregulation of cardiogenesis, cardiac conduction, and cell cycle in mice lacking miRNA-1-2. *Cell* 129:303–317.
54. Pall GS, et al. (2007) Carbodiimide-mediated cross-linking of RNA to nylon improves the detection of siRNA, miRNA, and piRNA by northern blot. *Nucleic Acids Res* 35: e60.
55. Valoczi A, et al. (2004) Sensitive and specific detection of microRNAs by northern blot analysis using LNA-modified oligonucleotide probes. *Nucleic Acids Res* 32:e175.